

YTHDF1 promotes the viability and self-renewal of glioma stem cells by enhancing LINC00900 stability

YUANHAI ZHANG^{1*}, YI ZHU^{2,3*}, YATING ZHANG^{2,3}, ZIXIANG LIU^{3,4} and XUDONG ZHAO^{1,2,3,4,5}

¹Department of Neurosurgery, The Affiliated Wuxi No. 2 People's Hospital of Nanjing Medical University, Wuxi, Jiangsu 214000; ²Department of Neurosurgery, Medical School of Nantong University, Nantong University, Nantong, Jiangsu 226019; ³Department of Neurosurgery, Wuxi No. 2 People's Hospital, Affiliated Wuxi Clinical College of Nantong University, Wuxi, Jiangsu 214000; ⁴Department of Neurosurgery, Jiangnan University Medical Center; ⁵Wuxi Neurosurgical Institute, Wuxi, Jiangsu 214002, P.R. China

Received September 20, 2023; Accepted February 23, 2024

DOI: 10.3892/ijo.2024.5641

Abstract. YTHDF1, an N6-methyladenosine (m6A)-binding protein, is significantly upregulated in glioma tissues. The present study investigated the molecular mechanism underlying the regulatory effects of YTHDF1 on the viability, invasion and self-renewal of glioma stem cells (GSCs). Glioma and normal brain tissues were collected, and reverse transcription-quantitative PCR and western blotting were used to measure the gene and protein expression levels, respectively. Methylated RNA immunoprecipitation-PCR was used to assess the m6A modification level of the target gene. Subsequently GSCs were induced, and YTHDF1 and LINC00900 gene regulation was carried out using lentiviral infection. The viability, invasion and self-renewal of GSCs were assessed by Cell Counting Kit-8, Transwell and sphere formation assays, respectively. Binding between YTHDF1 and LINC00900 was verified by RNA immunoprecipitation and RNA pull-down assays. The targeted binding of microRNA (miR)-1205 to the LINC00900/STAT3 3'-UTR was verified using a luciferase reporter assay. The results revealed that YTHDF1 and LINC00900 expression levels were significantly upregulated in glioma tissues, and a high m6A modification level in LINC00900 transcripts was detected in glioma tissues. Overexpression of YTHDF1 promoted GSC viability, invasion and self-renewal, whereas knockdown of YTHDF1 had the opposite effects. In addition, YTHDF1 maintained the stability of LINC00900 and upregulated its expression through binding to it, thereby promoting GSC viability, invasion

and self-renewal. Furthermore, LINC00900 promoted GSC viability, invasion, self-renewal and tumor growth by regulating the miR-1205/STAT3 axis. In conclusion, YTHDF1 promotes GSC viability and self-renewal by regulating the LINC00900/miR-1205/STAT3 axis.

Introduction

Glioma is one of the most common types of brain tumor, the main treatment methods for which include surgical resection, radiotherapy and chemotherapy (1). However, because of tumor recurrence, and resistance to radiotherapy and chemotherapy, most patients have a poor prognosis, with a median overall survival time of 14.6-20.5 months worldwide (2). Glioma recurrence and drug resistance are closely related to glioma stem cells (GSCs) (3). Therefore, the present study aimed to assess the characteristics and functions of GSC, which may further reveal the causes of glioma occurrence, development and recurrence, and provide novel ideas for treatment.

N6-methyladenosine (m6A) is the most abundant internal modification on RNA. It is dynamically and reversibly regulated by methyltransferases and demethylases. m6A affects the processing and metabolism of RNA, and regulates gene expression by binding to m6A-reading proteins (4,5). Abnormal m6A methylation on RNA is closely related to the occurrence and development of glioma (6,7). Cui *et al* (8) and Visvanathan *et al* (9) revealed that METTL3, METTL14 and FTO participate in regulating GSC self-renewal and tumorigenesis. Recent research has shown that knockdown of METTL3 reduces the self-renewal and proliferation of GSCs (10,11), indicating that m6A methylation serves a major role in regulating the self-renewal of GSCs. YTHDF1 is an m6A-binding protein that mediates m6A modification. In addition, YTHDF1 maintains mRNA stability (12-14) and enhances mRNA translation (15,16). Notably, YTHDF1 is significantly upregulated in glioma tissues (17). Knockdown of YTHDF1 has been shown to significantly inhibit glioblastoma (GBM) cell spheroidization, invasion, and the expression of GSC markers CD133, NANOG and OCT4 (18). However, the molecular mechanism underlying the regulatory effects of YTHDF1 on GSC self-renewal and invasion remains unclear.

Correspondence to: Dr Xudong Zhao, Department of Neurosurgery, The Affiliated Wuxi No. 2 People's Hospital of Nanjing Medical University, 68 Zhongshan Road, Wuxi, Jiangsu 214000, P.R. China
E-mail: zhaoxudong623@163.com

*Contributed equally

Key words: glioma, self-renewal, YTHDF1, LINC00900, N6-methyladenosine, RNA

Long non-coding RNA (lncRNA) is a type of RNA that contains >200 nucleotides, which has a major regulatory role in the process of tumorigenesis through various molecular mechanisms (19). m6A is distributed on mRNA and widely distributed on non-coding RNAs, such as lncRNA (20). Notably, m6A affects the occurrence and development of tumors by regulating the expression levels of lncRNAs (21); for example, m6A modification of lncDBET or DIAPH1-AS1 promotes the malignant progression of bladder cancer (22) or nasopharyngeal carcinoma growth and metastasis (23). LINC00900 is a newly discovered lncRNA. Wang *et al.* (24) detected high expression levels of LINC00900 in glioma, and revealed that LINC00900 is an m6A-related prognostic lncRNA for primary GBM. YTHDF1 reads m6A motifs and regulates the stability of the lncRNA THOR (25). Through preliminary research, it was revealed that multiple m6A methylation sites were detected on LINC00900 (SRAMP; <http://www.cuilab.cn/sramp>) and LINC00900 directly binds to YTHDF1 (m6A2Target; <http://rm2target.canceromics.org/#/home>) (Fig. S1), suggesting that YTHDF1 upregulates LINC00900 expression by maintaining its stability, and thus increases the viability and promotes self-renewal of GSCs.

The present study first investigated whether YTHDF1 regulates LINC00900 expression in an m6A-dependent manner, thereby promoting GSC viability, invasion and self-renewal. In addition, the mechanism by which LINC00900 upregulates STAT3 by sponging microRNA (miR)-1205 was verified, further promoting GSC activity, invasion, self-renewal and tumor growth. The present study aimed to assess whether YTHDF1/LINC00900 could be considered a potential therapeutic target for GBM.

Materials and methods

Clinical sample collection. Glioma tissues were collected from 20 patients admitted to Wuxi No. 2 People's Hospital (Wuxi, China) for surgical resection between January 2020 and January 2022. The 20 patients included 12 men and 8 women, aged between 26 and 70 years old, with an average age of 50.04 ± 12.34 (mean \pm SD) years. The patients did not receive radiotherapy, chemotherapy, targeted therapy or any other treatment that may affect the tumor, and did not have any other tumors or systemic diseases. A total of 16 patients had GBM [World Health Organization (WHO) grade IV] (26) and 4 patients had astrocytoma (WHO grade III). Additionally, 20 tumor-adjacent normal brain tissues (NBTs) were collected from the patients and were used as the control. The present study was approved by the Ethics Committee of Wuxi No. 2 People's Hospital (approval no. 2022-Y-116) and all patients provided written informed consent.

Serum-free induction of GSCs. The following human GBM cell lines were used: A172 (cat. no. CL-0012; Wuhan Punosai Life Technology Co., Ltd.), SHG44 (cat. no. BH-0109468; Shanghai Bohu Biotechnology Co., Ltd.), U87 MG (cat. no. FH0162; GBM of unknown origin) and U251 (cat. no. FH0159) (both from FuHeng Biology). A172, SHG44 and U87-MG cells were cultured in Dulbecco's modified Eagle's medium (DMEM; Gibco; Thermo Fisher Scientific, Inc.) supplemented with 10% fetal bovine serum (FBS; cat. no. F0193; Shanghai Noning

Biotechnology Co., Ltd.) and 100 U/ml penicillin/streptomycin (cat. no. G4003; Wuhan Servicebio Technology, Co., Ltd.) at 37°C with 5% CO₂. U251 cells were cultured in DMEM/F12 medium (Gibco; Thermo Fisher Scientific, Inc.) supplemented with 10% FBS and 100 U/ml penicillin/streptomycin at 37°C with 5% CO₂.

To induce differentiation, A172, SHG44, U87 MG and U251 cells were resuspended in neurobasal medium (cat. no. 21103049; Gibco; Thermo Fisher Scientific, Inc.) containing 20 ng/ml bFGF (cat. no. C046), 20 ng/ml EGF (cat. no. C029), 1 mg/ml heparin (cat. no. CK98) (all from Novoprotein Scientific, Inc.) and 100 U/ml penicillin/streptomycin. Cells were adjusted to 2×10^5 /ml for culture and neurobasal medium was replaced every 2-3 days. When the diameter of the glioma tumor spheres reached 150-200 μ m (after \sim 7 days), the glioma tumor spheres were collected and digested in an Accutase solution (cat. no. A6964; MilliporeSigma). A single cell suspension was prepared and subcultured.

Cell transfection/infection. The miR-1205 mimics and mimics negative control (NC) were synthesized by Shanghai GenePharma Co., Ltd., and 50 nM mimics were mixed with Lipofectamine[®] 2000 (Invitrogen; Thermo Fisher Scientific, Inc.) in OptiMEM (Gibco; Thermo Fisher Scientific, Inc.) to form complexes at room temperature, which were then transfected into the GSC-U87 and GSC-U251 cells at 37°C for a 2-3 day incubation, and RNA and protein extraction were performed after 48 h.

LINC00900/YTHDF1 overexpression/short hairpin RNA (shRNA) and control/shRNA-NC (sh-NC) lentiviruses (Plvx-shRNA2-mcherry-T2A-Puro and pGMLV-CMV-MCS-3xflag-EF1-Zsreen1-T2A-puro) were purchased from OLIGOBIO. To obtain cells with overexpression or knock down of LINC00900 and YTHDF1, GSC-U87 and GSC-U251 cells were infected with lentiviruses (MOI=10) at 37°C for 48 h, and cultured in medium supplemented with 5 μ g/ml puromycin after infection. The cells were collected for further experiments at 2 weeks post-infection. The sequences of the short hairpin (sh)RNAs and miRNA mimics are listed in Table I.

Reverse transcription-quantitative PCR (RT-qPCR). Total RNA was extracted from tissues or cells using an RNA extraction kit (cat. no. R1200; Shanghai Yuduo Biotechnology Co., Ltd.) in accordance with the manufacturer's instructions, and the RNA concentration was measured using an ultraviolet spectrophotometer. The extracted RNA was then reverse transcribed into cDNA using a RT kit according to manufacturer's protocol (cat. no. PC1703; Aidlab Biotechnologies Co., Ltd.), followed by qPCR analysis using a SYBR Green PCR kit (cat. no. PC3302; Aidlab Biotechnologies Co., Ltd.). The qPCR thermocycling conditions were as follows: Denaturation at 94°C for 30 sec; followed by 30-35 cycles of denaturation at 94°C for 30 sec, annealing at 55-60°C for 30 sec, and extension at 72°C for 24 sec; and a final extension step at 72°C for 5-10 min. The 2^{- $\Delta\Delta$ C_q} method (27) was used to analyze the relative expression levels of the target gene, and GAPDH was used as endogenous control. Primer sequences are listed in Table II.

Table I. Sequences of the shRNAs and miRNA mimics.

shRNA/mimics	Target sequence, 5'-3'
sh-LINC00900-1	CCTGGCTAGTCAATCTTTATT
sh-LINC00900-2	GAGGGTCCAAGGTTGTTATTT
sh-LINC00900-3	GAGGTTACTGTGATGATTAATA
sh-NC2	CCTAAGGTTAAGTCGCCCTCGC
sh-YTHDF1-1	GTTCGTTACATCAGAAGGATA
sh-YTHDF1-2	CGCCGTCCATTGGATTCCTT
sh-YTHDF1-3	AACCTCCATCTTCGACGACTT
sh-NC1	TTCTCCGAACGTGTCACGT
miR-1205 mimics	UCUGCAGGGUUUGCUUUGAG
Mimics NC	UCACAACCUCCUAGAAAGAGU AGA

miR, microRNA; NC, negative control; sh, short hairpin.

Table II. Primer sequences

Gene	Primer sequence, 5'-3'
LINC00900 (human)	F: TGGTGTATGGATTGGATTTGGTAG R: CAGTGTCTTGGTCGAGTTGCTCTT
STAT3 (human)	F: TCAGTCAAAGCAGCAAAGAAGGAGG R: AGGATAGAGATAGACCAGTGGAGAC
YTHDF1 (human)	F: AAGTGAAGGGGAAGTTTGTATGT R: ATGGAGTTGTGTGCTTGTAGGA
GAPDH (human)	F: GGAGCGAGATCCCTCCAAAT R: GGCTGTTGTCATACTTCTCATGG
miR-1205	F: ACACTCCAGCTGGGTCTGCAGGGTT TGC R: CTCAACTGGTGTCTGGAGTCGGC AATTCAGTTGAGCTCAAAGC
U6	F: CTCGCTTCGGCAGCACAA R: AACGCTTACGAATTTGCGT

F, forward; miR, microRNA; R, reverse.

Western blotting. Total proteins were extracted from tissues or cells using RIPA buffer (cat. no. P0013B; Beyotime Institute of Biotechnology) in accordance with the manufacturer's instructions. A BCA kit (cat. no. BL521A; Biosharp Life Sciences) was used to measure the protein concentration. The proteins (25 µg) were then separated by SDS-PAGE (Mini-PROTEAN® 3 cell; Bio-Rad Laboratories, Inc.) on 8% gels and were transferred to a PVDF membrane (cat. no. IPVH00010; MilliporeSigma). Subsequently, 5% dry skim milk was used to block the membranes at room temperature for 3 h. The following primary antibodies were then applied at 4°C overnight: Anti-YTHDF1 (1:1,000; cat. no. ab220162; Abcam), anti-STAT3 (1:1,000; cat. no. ab68153; Abcam), anti-NANOG (1:1,000; cat. no. ab109250; Abcam), anti-OCT4 (1:1,000; cat. no. ab137427; Abcam) and anti-GAPDH (1:5,000; cat. no. 60004-1-Ig; Proteintech Group, Inc.), followed by the

secondary antibodies (1:5,000; cat. nos. ZB2301 and ZB2305; OriGene Technologies, Inc.) at room temperature for 2 h. Target protein bands were developed by enhanced chemiluminescence (cat. no. ECL-0011; Beijing Dingguo Changsheng Biotechnology Co., Ltd.) and detected using a chemiluminescence imager (ChemiScope 5300 Pro; Shanghai Huanxi Medical Equipment Co., Ltd.).

Methylated RNA immunoprecipitation (MeRIP)-PCR. Total RNA was extracted from tissues, and the Magna m6A RNA methylation immunoprecipitation kit (cat. no. C11051-1; Guangzhou Ruibo Biotechnology Co., Ltd.) was used for MeRIP in accordance with the manufacturer's instructions. The enriched RNA was then analyzed by RT-qPCR as aforementioned.

Identification of GSCs by immunofluorescence. The induced GSCs were collected, washed with PBS and fixed with 4% paraformaldehyde for 30 min at 4°C. Then, the anti-CD133 primary antibody (1:500; cat. no. 66666-1-Ig; Proteintech Group, Inc.) was applied at 4°C overnight. Subsequently, the corresponding Cy3-conjugated Affinipure Goat Anti-Mouse IgG (H+L) secondary antibody (1:80; cat. no. SA00009-1; Proteintech Group, Inc.) was applied at 37°C for 1 h and a Hoechst 33342 staining solution (10 µg/ml; cat. no. 875756-97-1; MilliporeSigma) was applied for 10 min at room temperature. CD133 immunofluorescence was observed under a fluorescence microscope (DP70; Olympus Corporation).

Cell viability assay. Suspensions of cells transfected with miRNA mimics or infected with LINC00926/YTHDF1 overexpression/knockdown lentiviruses were seeded in a 96-well plate at 2,000 cells/well. After 24 h, 10 µl Cell Counting Kit (CCK)-8 solution (cat. no. C0038; Beyotime Institute of Biotechnology) was added to each well for 2 h at 37°C. A microplate reader (MK3; Thermo Fisher Scientific, Inc.) was used to measure absorbance at 450 nm.

Transwell assay. GSCs (2×10^5) were collected and seeded in the upper chamber of a 24-well Transwell system (pore size, 8 µm) precoated with Matrigel (cat. no. 354234; Shanghai Yanhui Biotechnology Co., Ltd.) at 37°C for 1 h, and culture medium containing 10% FBS was added to the lower chamber. Cells were incubated for 24 h at 37°C, and then the medium in the upper chamber was discarded. Cells were fixed with 4% 40 g/l paraformaldehyde for 15 min at 4°C, washed with PBS and then stained with 0.2% crystal violet at room temperature for 5 min. Cells on the bottom membrane of the chamber were gently wiped with a cotton swab. After drying, the chamber was observed under an optical microscope (DFC300 FX; Leica Microsystems, Inc.) and cells were counted.

Tumor sphere formation assay. A total of 2,000 GSCs/well were seeded in the well of a 24-well plate in medium supplemented with 20 mg/ml B27 (cat. no. 17504044; Gibco; Thermo Fisher Scientific, Inc.), 20 ng/ml EGF and 20 ng/ml bFGF. EGF and bFGF were added to the medium twice a week. After 2-3 weeks of culture, the number of spheres formed in each well was observed under an optical microscope. Sphere formation efficiency (SFE) was used to evaluate stem cell self-renewal, as

follows: SFE=number of cell spheres with a >75 μm diameter per well/total number of original seeded cells in per well.

RNA pull-down assay. GSC-U87 and GSC-U251 cells were lysed using IP lysis solution (cat. no. ZN2923; Beijing Baiao Leibo Technology Co., Ltd.) on ice for 15 min and the supernatant was collected by centrifugation (4°C, 16,000 x g, 10 min). The biotin-labeled LINC00900 probe and negative control probe were synthesized by Guangzhou RiboBio Co., Ltd. Subsequently, 0.4 μg (50 pmol) biotin-labeled RNA was incubated with 0.5 ml cell lysate at 4°C for 1 h. Then, 50 μl protein G agarose beads were added and incubated at 4°C for 1 h. Agarose beads were centrifuged at 13,400 x g, for 30 sec at 4°C for precipitation and the supernatant was collected into a clean tube. After washing, western blotting was performed to detect the target protein as aforementioned.

RNA immunoprecipitation (RIP). RIP was conducted using a RIP kit [cat. no. GS-ET-006; Genseq; Hylegen Biotechnology (Shanghai) Co., Ltd.] in accordance with the manufacturer's instructions. Cells were lysed using 250 μl complete lysis buffer for 5 min, and 50 μl lysate was then incubated with IgG (1:100, cat. no. 36111ES10) or an anti-YTHDF1 antibody (1:500; cat. no. 31040ES50) (both from Shanghai Yeasen Biotechnology Co., Ltd.). RNA was extracted and purified, and RT-qPCR was used to measure target gene expression, as aforementioned.

RNA stability analysis. Cells infected with LV-sh-NC and LV-sh-YTHDF1 lentiviruses [Hanheng Biotechnology (Shanghai) Co., Ltd.] were seeded in 6-well plates. After 24 h of culture, the cells reached 70% confluence. The cells were then treated with 5 $\mu\text{g}/\text{ml}$ actinomycin D (cat. no. 1036; BioVision; Abcam) for 0, 2 or 4 h at 37°C, and the expression levels of LINC00900 were measured by RT-qPCR as aforementioned.

Luciferase reporter assay. Prediction analysis (DIANA-LncBase v.2, <http://diana.imis.athena-innovation.gr/DianaTools/index.php?r=site/page&view=software>; and TargetScan, https://www.targetscan.org/vert_71/) revealed a miR-1205-binding site in the LINC00900 transcript and STAT3 3'UTR. LINC00900 and STAT3 3'-UTR wildtype (WT) and mutant type (MUT) luciferase reporter genes (pmirGLO) were constructed by Beijing Olinger Biotechnology Co., Ltd. and co-transfected with miR-1205 mimics or mimics NC into 293T cells (cat. no. JN15568; Shanghai Jining Biotechnology Co., Ltd) by Lipofectamine 2,000. After 48 h, the dual luciferase reporter gene detection kit (cat. no. E1910; Promega Corporation) was used to detect the firefly luciferase activity and *Renilla* luciferase activity. The ratio of firefly luciferase to *Renilla* luciferase was calculated, and the control group was set as 1 to calculate the relative luciferase activity of different treatment groups.

Xenograft tumor model. Male nude specific pathogen-free mice (n=20; age, 3-4 weeks) were purchased from Beijing Huafukang Biotechnology Co., Ltd. The mice were maintained at 20-26°C and 50-60% relative humidity. They were supplied with *ad libitum* access to sufficient food/water and were kept under a 12-light/dark cycle. The nude mice were divided

into the following four groups (n=5/group): LV-sh-NC1 + LV-sh-NC2, LV-sh-YTHDF1, LV-sh-LINC00900 and LV-sh-YTHDF1 + LV-sh-LINC00900. All mice were subcutaneously injected with 5×10^6 GSC-U87 cells infected with LINC00900/YTHDF1 knockdown lentiviruses. After 1 week, the tumor growth curve and diameter were measured to calculate tumor volume ($1/2 \times \text{length} \times \text{width}^2$). All experiments were conducted in accordance with protocols approved by the Medical Ethics Committee of Wuxi No. 2 People's Hospital (Wuxi, China, approval no. 2023-Y-200).

If the animals reached any of the following humane endpoints they were sacrificed: The maximum tumor diameter exceeded 15 mm; animal weight loss reached $\leq 20\%$; the animal exhibited cachexia or wasting syndrome; the size of the solid tumor exceeded 10% of body weight. The experimental duration of the present study was 4 weeks, with the first week being used for adaptive feeding. At the beginning of the second week, the experiment was initiated (subcutaneous injection of GSCs to establish a xenograft tumor animal model) and animal status was observed daily. Tumor volume was measured from the first week after tumor cell injection, every 3 days for 2 weeks. Notably, none of the mice succumbed during the experimental process. At the end of the experiment, the mice were euthanized using CO₂ (100% CO₂, 20 l/min; total chamber volume, 40 l; displacement rate, 50% l/min), and to verify death, breathing was assessed. In the present study, all nude mice showed a maximum weight loss of <15% before euthanasia.

Immunohistochemistry. After tumor formation, animals were euthanized, and tumor tissues were harvested. The tumor tissues were fixed in 4% paraformaldehyde at 4°C for 24 h and 4- μm paraffin-embedded sections were prepared. The paraffin-embedded sections were dehydrated in a descending series of ethanol, followed by antigen repair with sodium citrate at 95-100°C, and blocking with H₂O₂ at room temperature for 5-10 min and goat serum (cat. no. 16210064; Thermo Fisher Scientific, Inc.) at room temperature for 10 min. The sections were then stained with an anti Ki-67 antibody (1:100; cat. no. TA500265; OriGene Technologies, Inc.) at 4°C overnight and with a biotin-labeled secondary antibody (cat. no. SAP-9100; OriGene Technologies, Inc.) at 37°C for 30 min. After washing, Ki-67 staining was observed under an optical microscope, and image analysis software (ImageJ v1.8.0; National Institutes of Health) was used to semi-quantitatively evaluate the intensity and degree of Ki-67 staining.

TUNEL assay. The aforementioned paraffin-embedded tumor tissue sections were subjected to apoptosis detection using the TUNEL cell apoptosis assay kit (cat. no. C1091; Beyotime Institute of Biotechnology) according to the manufacturer's instructions. Under an optical microscope, five fields of view were observed. And the brown yellow staining represented apoptotic cells. Apoptosis rate was calculated as number of positive cells/total number of cells.

Statistical analysis. GraphPad Prism 5 software (Dotmatics) was used for statistical analysis. Each experiment was performed at least in triplicate, and the data are presented

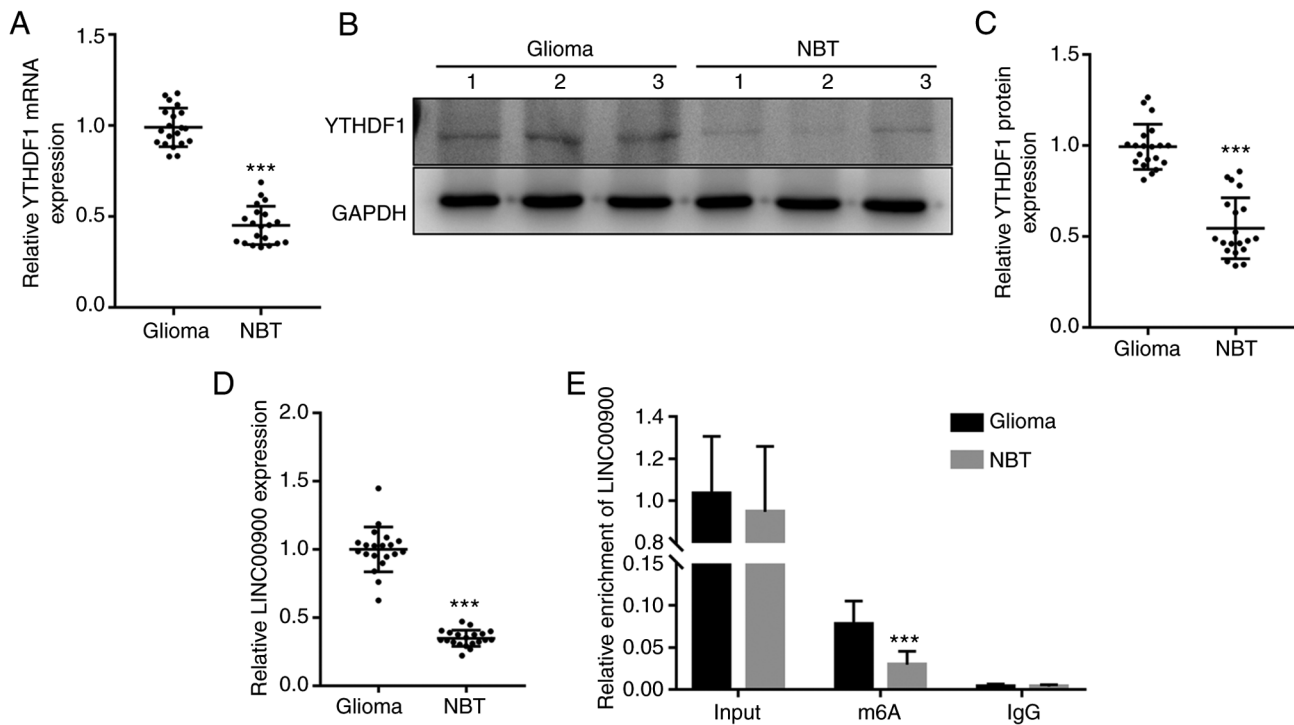


Figure 1. Abnormal expression of YTHDF1 and LINC00900 in glioma tissue. Glioma tissues were collected from 20 patients with glioma, and 20 NBTs were obtained from patients undergoing internal decompression for treatment of brain trauma as the control. (A) RT-qPCR was used to measure YTHDF1 mRNA expression in glioma tissues and NBTs. (B) Western blotting was used to measure YTHDF1 protein expression in glioma tissues and NBTs. (C) Histogram of relative expression levels of YTHDF1 protein in glioma tissues and NBTs. (D) Measurement of LINC00900 expression in glioma tissues and NBTs by RT-qPCR. (E) Measurement of the m6A modification level of LINC00900 in tumor tissues and NBTs by methylated RNA immunoprecipitation-PCR. Data are presented as the mean \pm SD. *** P <0.001 vs. glioma. m6A, N6-methyladenosine; NBT, normal brain tissue; RT-qPCR, reverse transcription-quantitative PCR.

as the mean \pm SD. Comparisons between two groups were performed using a two-tailed unpaired Student's *t*-test, and multiple groups were analyzed by one-way ANOVA followed by Tukey's post hoc test or mixed ANOVA followed by Bonferroni's post hoc test. P <0.05 was considered to indicate a statistically significant difference.

Results

Abnormal expression of YTHDF1 and LINC00900 in glioma tissue. RT-qPCR and western blotting were performed to measure the expression levels of YTHDF1 in glioma tissue and NBT. RT-qPCR showed that the mRNA expression levels of YTHDF1 were significantly upregulated in glioma tissue (Fig. 1A). Consistent with the trend in gene expression, the protein expression levels of YTHDF1 in glioma tissues were also significantly higher than those in NBTs (Fig. 1B and C). Subsequently, RT-qPCR was conducted to measure the expression levels of LINC00900 in glioma tissue and NBT. As shown in Fig. 1D, the expression levels of LINC00900 in glioma tissues were significantly higher than those in NBTs. A total of 16 patients had GBM (WHO grade IV) (26) and 4 patients had astrocytoma (WHO grade III). As shown in Fig. S2, LINC00900 expression in the glioma tissues of the two groups was significantly higher than that in the adjacent tissues, and no significant difference was found in the expression of LINC00900 between the two groups. Subsequently, MeRIP-PCR analysis revealed that the LINC00900 transcript in glioma tissues was enriched with m6A (Fig. 1E), suggesting

that the high content of m6A in LINC00900 transcripts may be the cause of its abnormal expression in glioma tissue.

Overexpression of YTHDF1 promotes viability, invasion and self-renewal of GSCs. Four glioma cell lines (A172, U87, U251 and SHG44) were selected to induce GSCs. GSCs were generated by serum-free induction and, as shown in Fig. S3A, stem cells were successfully induced and named GSC-U87 and GSC-U251. GSC-A172 and GSC-SHG44 cells were also induced and are shown in Fig. S4A. The GSCs were identified by immunofluorescence (Figs. S3B and S4B), and western blotting (Fig. S3C) of the stem cell markers CD133, NANOG and OCT4. RT-qPCR and western blotting showed that compared with that in A172, U87, U251 and SHG44 cells, YTHDF1 expression levels in GSC-A172, GSC-U87, GSC-U251 and GSC-SHG44 cells were significantly increased (Fig. 2A and B). U251 and U87 cells are two commonly used glioma cell lines for *in vitro* experiments, which were isolated from GBM and are often used as an *in vitro* model of GBM. Therefore, these cell lines were selected to study the effects of YTHDF1 on the viability, invasion and self-renewal of GSCs. Subsequently, GSC-U87 and GSC-U251 cells were infected with YTHDF1 overexpression or knockdown lentiviruses. As shown in Fig. 2C-E, YTHDF1 overexpression significantly upregulated YTHDF1 mRNA and protein expression levels, whereas YTHDF1 knockdown significantly downregulated YTHDF1 mRNA and protein expression levels in GSC-U87 and GSC-U251 cells. Notably, shRNA-2 had the best knockdown efficiency, and was therefore used

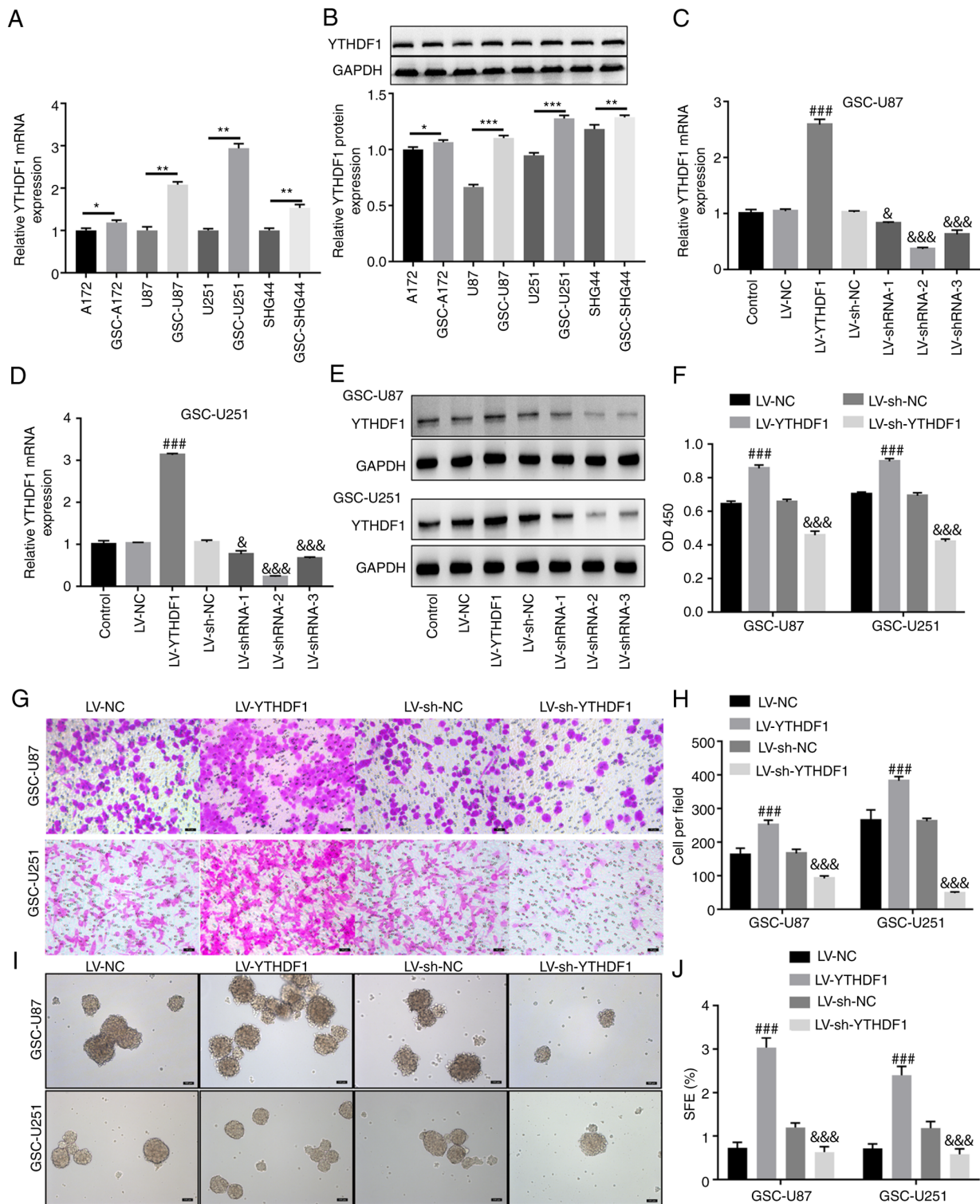


Figure 2. Overexpression of YTHDF1 promotes the viability, invasion and self-renewal of GSCs. YTHDF1 overexpression and LV-mediated knockdown were applied to GSC-U87 and GSC-U251 cells. (A) RT-qPCR and (B) western blotting was used to measure the protein expression levels of YTHDF1 in U87, U251, GSC-U87 and GSC-U251 cells. Overexpression and knockdown efficiencies assessed by RT-qPCR in (C) GSC-U87 and (D) GSC-U251 cells. (E) Overexpression and knockdown efficiencies assessed by western blotting. (F) Cell Counting Kit-8 assay of GSC viability. (G) Transwell assay of GSC invasion. Scale bars, 50 μ m. (H) Histogram of the number of invasive GSCs. (I) Tumor sphere formation assay evaluated the self-renewal capability of GSCs. Scale bars, 100 μ m. (J) Histogram of the sphere formation efficiency of GSCs. Data are presented as the mean \pm SD. * P <0.05 vs. A172, ** P <0.01, *** P <0.001 vs. U87 or U251 or SHG44, ### P <0.001 vs. LV-NC; & P <0.05, &&& P <0.001 vs. LV-sh-NC. GSCs, glioma stem cells; LV, lentivirus; NC, negative control; RT-qPCR, reverse transcription-quantitative PCR; SFE, sphere formation efficiency; sh, short hairpin.

in subsequent experiments. The results of a CCK-8 assay showed that YTHDF1 overexpression significantly increased GSC-U87 and GSC-U251 cell viability, whereas knockdown

of YTHDF1 significantly decreased GSC-U87 and GSC-U251 cell viability (Fig. 2F). The Transwell assay showed that YTHDF1 overexpression significantly increased the invasive

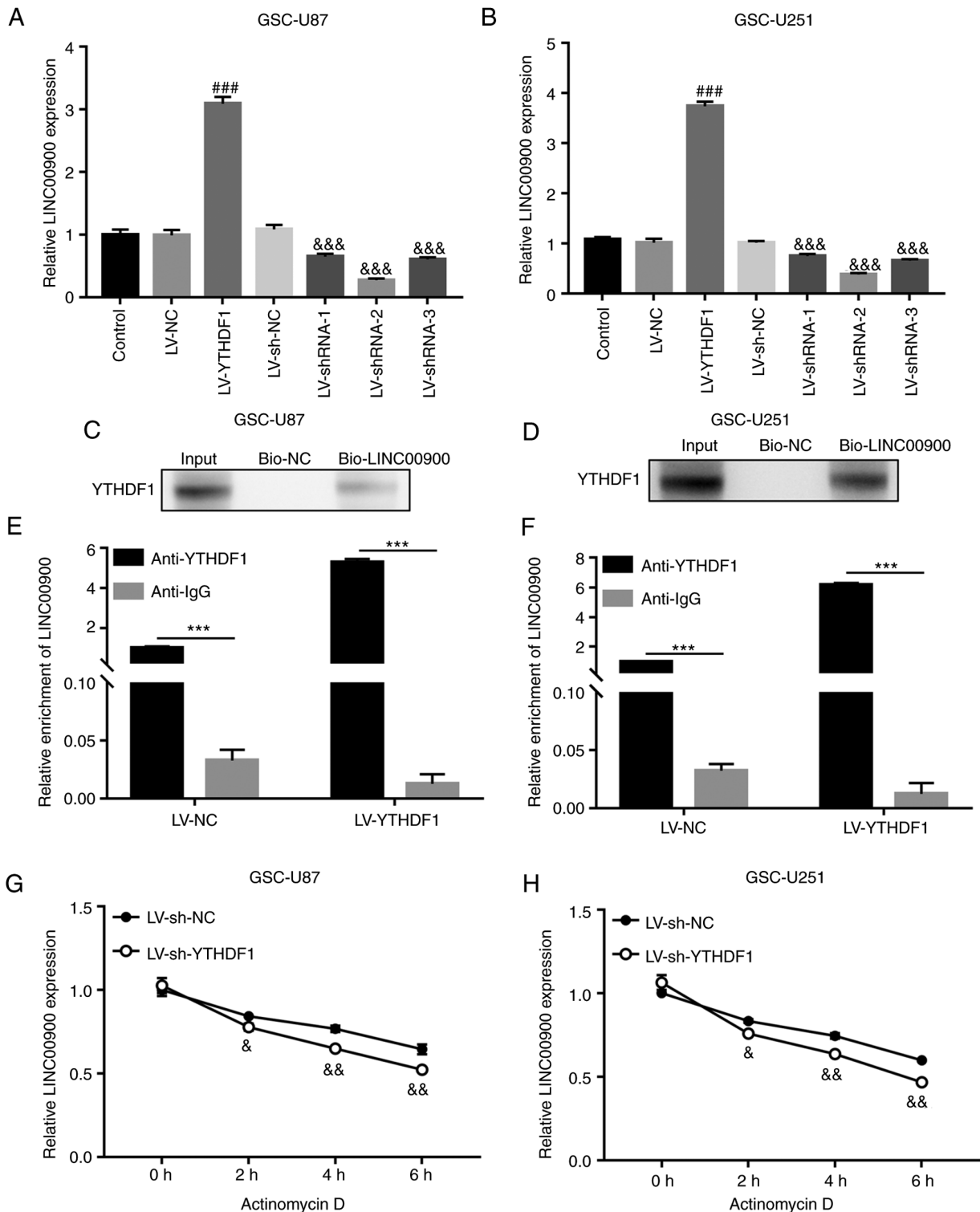


Figure 3. YTHDF1 upregulates LINC00900 expression by enhancing its stability. GSC-U87 and U251 cells were infected with LVs for YTHDF1 overexpression or knockdown. LINC00900 expression was measured by RT-qPCR in (A) GSC-U87 and (B) GSC-U251 cells. RNA pull-down assays demonstrated direct binding of YTHDF1 protein to LINC00900 in (C) GSC-U87 and (D) GSC-U251 cells. RNA immunoprecipitation assay indicated that YTHDF1 protein bound directly to LINC00900 in (E) GSC-U87 and (F) GSC-U251 cells. Using actinomycin D, the stability of LINC00900 was evaluated by RT-qPCR in (G) GSC-U87 and (H) GSC-U251 cells. Data are presented as the mean \pm SD. ### P <0.001 vs. LV-NC, *** P <0.001, * P <0.05, && P <0.01, &&& P <0.001 vs. LV-sh-NC. GSC, glioma stem cell; LV, lentivirus; NC, negative control; RT-qPCR, reverse transcription-quantitative PCR; sh, short hairpin.

ability of GSC-U87 and GSC-U251 cells, whereas knockdown of YTHDF1 significantly decreased the invasive ability of GSC-U87 and GSC-U251 cells (Fig. 2G and H). The tumor sphere formation assay showed that YTHDF1 overexpression significantly increased the tumor sphere formation ability

of GSC-U87 and GSC-U251 cells, whereas knockdown of YTHDF1 significantly decreased the tumor sphere formation ability of GSC-U87 and GSC-U251 cells (Fig. 2I and J). These results suggested that YTHDF1 overexpression promoted the viability, invasion and self-renewal of GSCs.

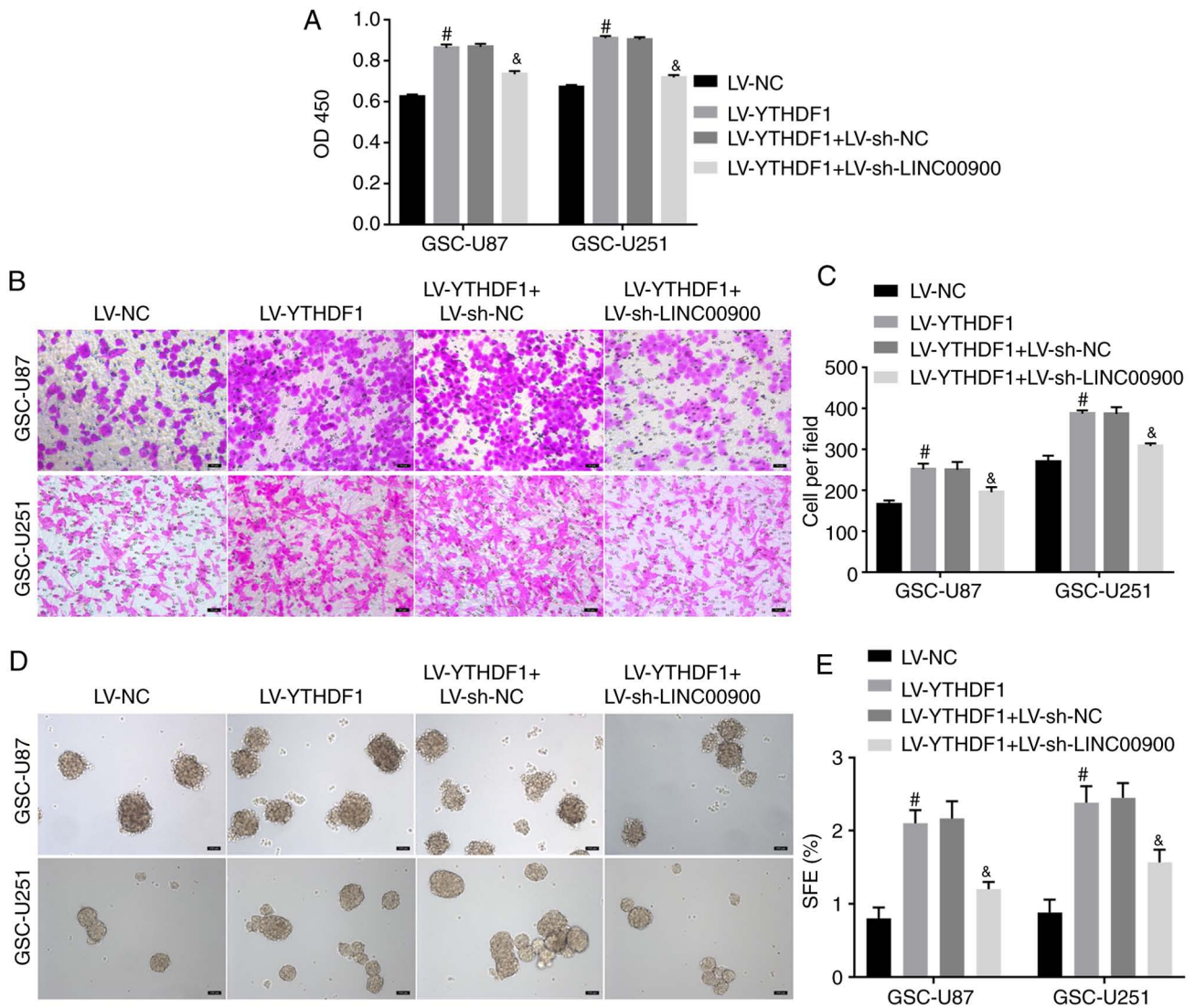


Figure 4. YTHDF1 promotes GSC viability, invasion and self-renewal by upregulating LINC00900 expression. GSC-U87 and GSC-U251 cells were co-infected with LVs for YTHDF1 overexpression and LINC00900 knockdown. (A) Cell Counting Kit-8 assay of GSC viability. (B) Transwell assay of GSC invasion. Scale bars, 50 μ m. (C) Histogram of the number of invasive GSCs. (D) Tumor sphere formation assay was used to evaluate the self-renewal capability of GSCs. Scale bars, 100 μ m. (E) Histogram of the sphere formation efficiency of GSCs. Data are presented as the mean \pm SD. [#] $P < 0.05$ vs. LV-NC; [&] $P < 0.05$ vs. LV-YTHDF1 + LV-sh-NC. GSC, glioma stem cell; LV, lentivirus; NC, negative control; SFE, sphere formation efficiency; sh, short hairpin.

YTHDF1 upregulates LINC00900 expression by enhancing its stability. To investigate whether YTHDF1 affects the expression of LINC00900, YTHDF1 overexpression or knockdown was performed in GSC cells. The results showed that the expression levels of LINC00900 were increased in YTHDF1-overexpressing GSCs and were decreased in YTHDF1-knockdown GSCs (Fig. 3A and B). RNA pull-down and RIP assays were used to demonstrate the binding of the YTHDF1 protein to LINC00900 in GSCs. As shown in Fig. 3C and D, the RNA pull-down assay showed that the biotin-labeled LINC00900 (bio-LINC00900) pull-down complex contained YTHDF1 protein. Moreover, in the RIP assay, LINC00900 was detected in the YTHDF1 antibody pull-down complex. In addition, there was a significant difference between anti-YTHDF1 and IgG groups, indicating that the enrichment of LINC00900 on the YTHDF1 protein was significantly increased (Fig. 3E and F). These results identified the binding relationship between LINC00900 and YTHDF1. Actinomycin D can be absorbed by cells within a few minutes

and preferentially embedded into DNA sequences rich in GC, forming stable complexes that inhibit the transcription process of all eukaryotic RNA polymerase enzymes. After treating with actinomycin D for different durations, the molecular level of target RNA (such as mRNA and lncRNA) can be detected, the half-life of the target RNA can be calculated, and its stability evaluated. Using actinomycin D, it was revealed that LINC00900 expression was significantly reduced in YTHDF1-knockdown GSCs (Fig. 3G and H), indicating that YTHDF1 affected LINC00900 expression by regulating its stability.

YTHDF1 promotes GSC viability, invasion and self-renewal by upregulating LINC00900 expression. To further explore whether YTHDF1 regulates LINC00900 expression and affects GSC functions, YTHDF1 was overexpressed and LINC00900 was knocked down. Fig. S5A and B shows successful knockdown of LINC00900 in GSC-U87 and GSC-U251 cells. The results of a CCK-8 assay showed that YTHDF1 overexpression

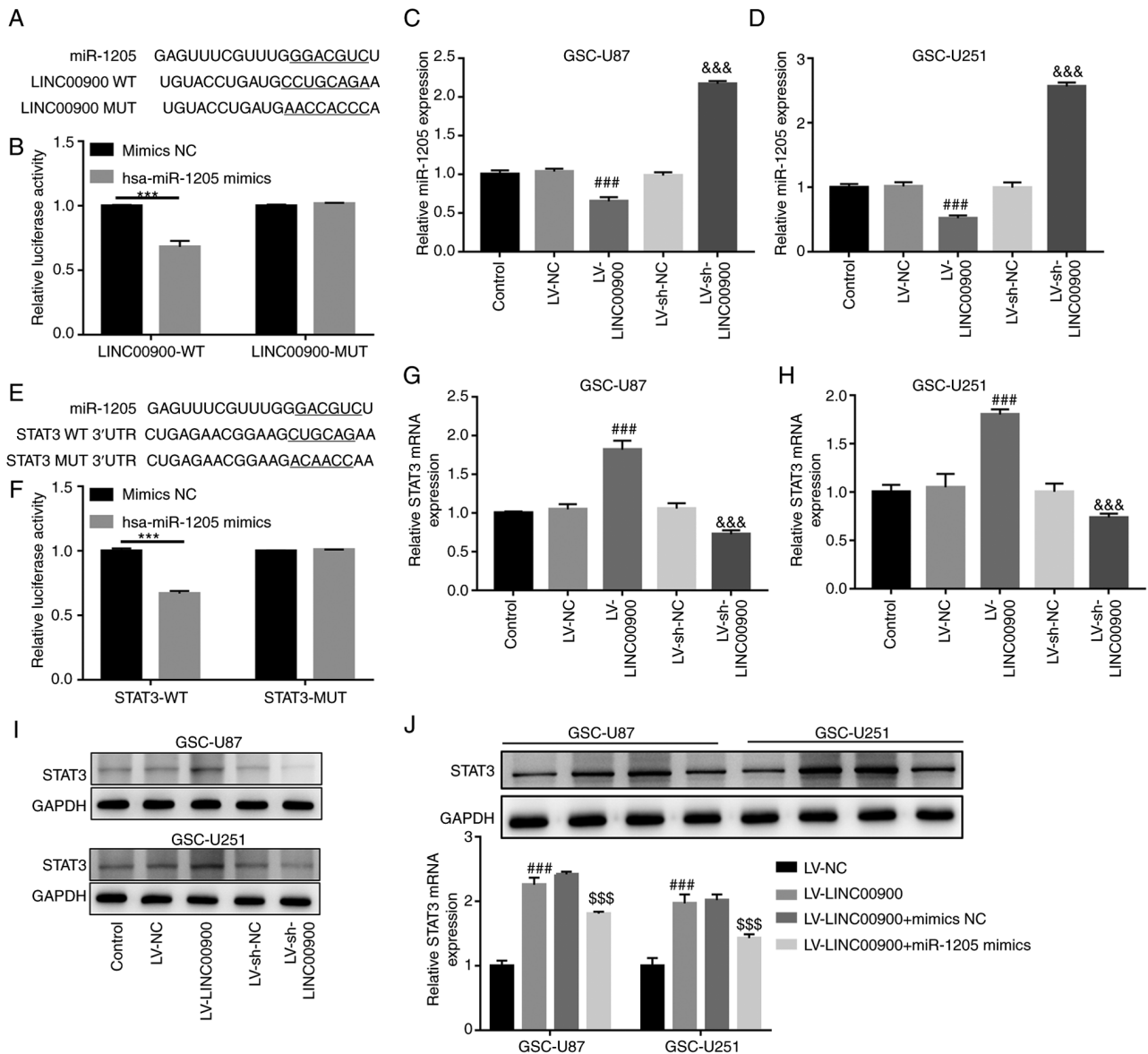


Figure 5. LINC00900 upregulates STAT3 expression by sponging miR-1205. (A) A miR-1205-binding site on the LINC00900 transcript. (B) Luciferase assay of LINC00900 and miR-1205-binding sites was used to verify their regulatory relationship. GSC-U87 and GSC-U251 cells were infected with LVs for LINC00900 overexpression or knockdown. The miR-1205 expression levels were measured by RT-qPCR in (C) GSC-U87 and (D) GSC-U251 cells. (E) A miR-1205-binding site on the STAT3 3'UTR. (F) Luciferase assay was used to verify the direct binding of miR-1205 to the STAT3 3'UTR and their regulatory relationship. GSC-U87 and GSC-U251 cells were infected with LVs for LINC00900 overexpression or knockdown. STAT3 mRNA expression was measured by RT-qPCR in (G) GSC-U87 (H) GSC-U251 cells. (I) STAT3 protein expression levels were measured by western blotting. (J) LINC00900 and miR-1205 were co-overexpressed in GSC-U87 and GSC-U251 cells. STAT3 mRNA and protein expression levels were then measured by RT-qPCR and western blotting, respectively. Data are presented as the mean \pm SD. *** P <0.001 as indicated; \$\$\$ P <0.001 vs. LV-LINC00900 + mimics NC; ### P <0.001 vs. LV-NC; &&& P <0.001 vs. LV-sh-NC. GSC, glioma stem cell; LV, lentivirus; miR, microRNA; MUT, mutant; NC, negative control; RT-qPCR, reverse transcription-quantitative PCR; sh, short hairpin; WT, wild type.

promoted viability, whereas knockdown of LINC00900 reversed the enhancing effect of YTHDF1 on viability (Fig. 4A). The Transwell assay showed that knockdown of LINC00900 reversed the effect of YTHDF1 on GSC invasion (Fig. 4B and C). The tumor sphere formation assay showed that knockdown of LINC00900 reversed the effect of YTHDF1 on GSC tumor sphere formation (Fig. 4D and E). These data indicated that YTHDF1 promoted GSC viability, invasion and self-renewal by upregulating LINC00900 expression.

LINC00900 upregulates STAT3 expression by sponging miR-1205. Prediction analysis using LncBase v.2 revealed

a miR-1205-binding site on the LINC00900 transcript (Fig. 5A). miR-1205 expression was revealed to be significantly decreased in glioma tissue compared with that in NBT (Fig. S6A). The luciferase reporter assay confirmed the target binding relationship between miR-1205 and LINC00900 (Fig. 5B). Subsequently, LINC00900 was successfully overexpressed in GSC-U251 and GSC-U87 cells (Fig. S5A and B). The results revealed that LINC00900 overexpression significantly inhibited miR-1205 expression, whereas knockdown of LINC00900 upregulated miR-1205 expression (Fig. 5C and D), implying that LINC00900 negatively regulated miR-1205 expression.

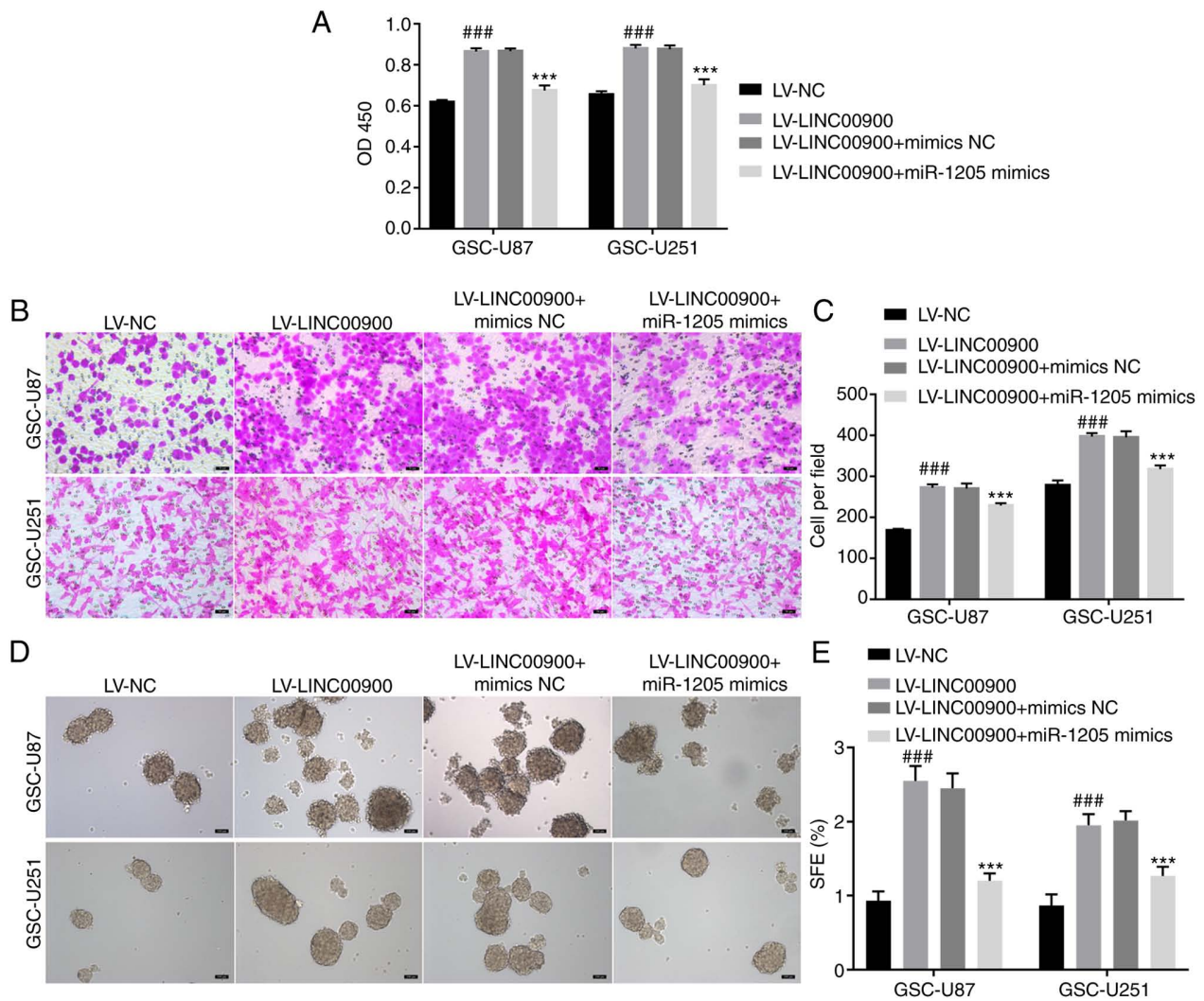


Figure 6. LINC00900 promotes GSC viability, invasion and self-renewal by regulating the miR-1205/STAT3 axis. LINC00900 and miR-1205 were co-overexpressed in GSC-U87 and GSC-U251 cells. (A) Cell Counting Kit-8 assay of GSC viability. (B) Transwell assay of GSC invasion. Scale bars, 50 μ m. (C) Histogram of the number of invasive GSCs. (D) Tumor sphere formation assay was used to evaluate the self-renewal capability of GSCs. Scale bars, 100 μ m. (E) Histogram of the sphere formation efficiency of GSCs. Data are presented as the mean \pm SD. ^{###} $P < 0.001$ vs. LV-NC; ^{***} $P < 0.001$ vs. LV-LINC00900 + mimics NC. GSC, glioma stem cell; LV, lentivirus; miR, microRNA; NC, negative control; SFE, sphere formation efficiency; sh, short hairpin.

Prediction analysis using TargetScan also revealed a miR-1205-binding site on the STAT3 3'-UTR (Fig. 5E). The mRNA and protein expression levels of STAT3 were significantly increased in glioma tissue compared with those in NBT (Fig. S6B and C). The luciferase reporter assay confirmed the target binding relationship between miR-1205 and the STAT3 3'-UTR (Fig. 5F). In addition, it was revealed that LINC00900 overexpression significantly upregulated STAT3 expression, whereas knockdown of LINC00900 inhibited STAT3 expression (Fig. 5G-I), implying that LINC00900 positively regulated STAT3 expression. Furthermore, LINC00900 and miR-1205 were overexpressed in GSCs. Fig. S5C and D show successful overexpression of miR-1205 in GSC-U87 and GSC-U251 cells. The miR-1205 mimics reversed the upregulating effect of LINC00900 on STAT3 expression (Fig. 5J), which indicated that LINC00900 may upregulate STAT3 expression by sponging miR-1205.

LINC00900 promotes GSC viability, invasion, self-renewal and tumor growth by regulating the miR-1205/STAT3

axis. To further explore whether LINC00900 regulates the miR-1205/STAT3 axis and thus affects GSC functions, LINC00900 and miR-1205 were overexpressed in GSCs. The transfection efficiency of LINC00900 and miR-1205 is shown in Fig. S5. The results of a CCK-8 assay showed that LINC00900 overexpression promoted viability, whereas the miR-1205 mimics reversed the inducing effect of LINC00900 on cell viability (Fig. 6A). The Transwell assay showed that the miR-1205 mimics reversed the effect of LINC00900 on GSC invasion (Fig. 6B and C). The tumor sphere formation assay showed that the miR-1205 mimics also reversed the effects of LINC00900 on GSC tumor sphere formation (Fig. 6D and E).

Analysis of xenografted tumors in nude mice showed that inhibition of YTHDF1 or LINC00900 slowed tumor growth rate, and the tumor volume and weight of the simultaneous YTHDF1 and LINC00900 inhibition group were lower than those in the single inhibition groups (Fig. 7A-C). Compared with tumors in the LV-sh NC1 + LV-sh NC2 group mice, miR-1205 expression was increased in tumors in the LV-sh-YTHDF1 and LV-sh-LINC00900 group mice, whereas STAT3 expression was reduced (Fig. 7D and E).

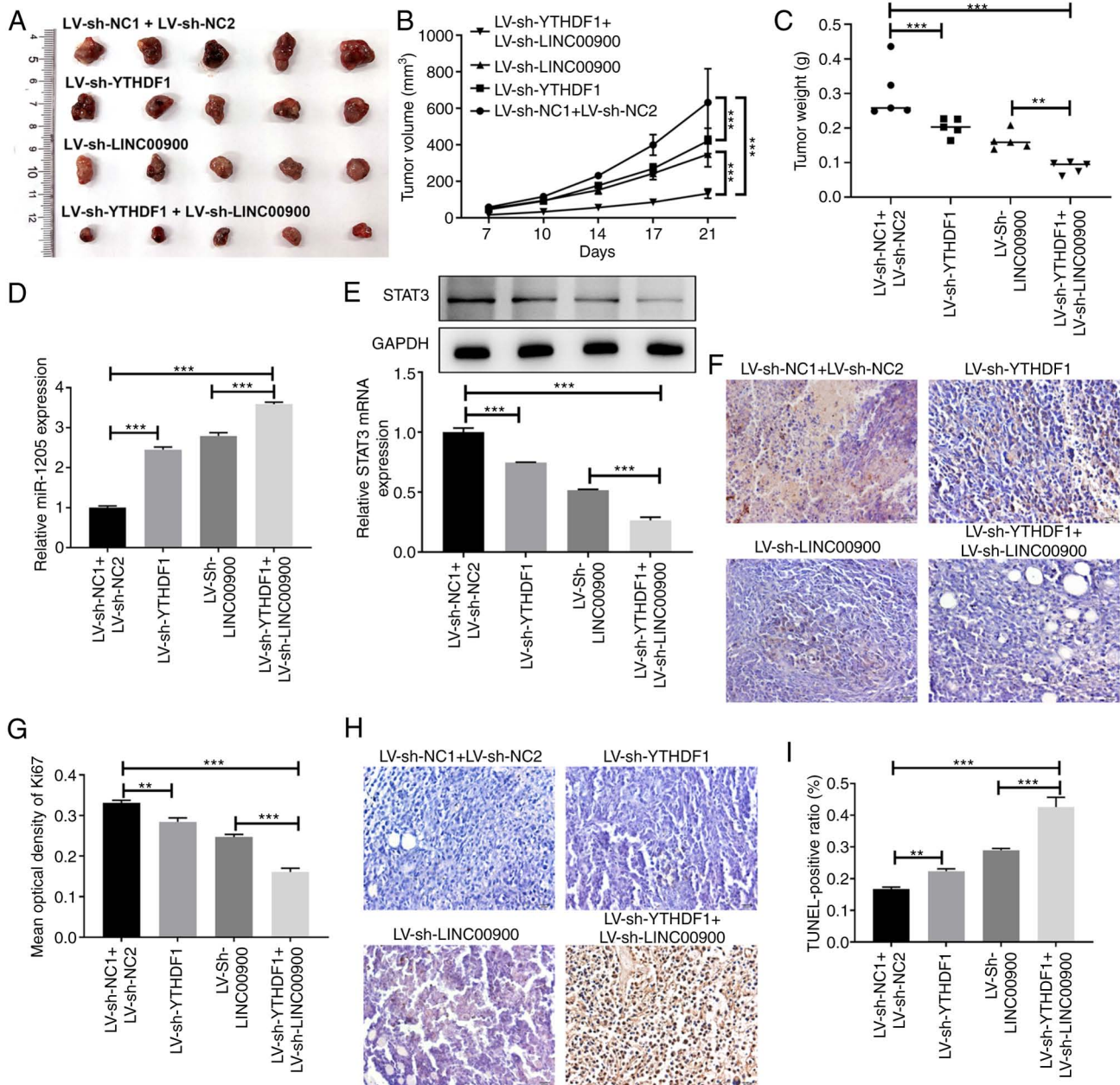


Figure 7. LINC00900 promotes glioma stem cell tumor growth by regulating the miR-1205/STAT3 axis. (A) Representative images of xenografted tumors. (B) Growth curves of xenografted tumors in nude mice. (C) Tumor weight. (D) Relative expression levels of miR-1205 in xenografted tumors were examined by RT-qPCR. (E) Relative expression levels of STAT3 in xenografted tumors were examined by RT-qPCR and western blotting. (F) Analysis of cell proliferation in tumor tissue by Ki-67 staining (magnification, x400). (G) Histogram of Ki-67 staining. (H) Analysis of apoptosis in tumor tissues by TUNEL staining (magnification, x400). (I) Histogram of TUNEL staining. Data are presented as the mean \pm SD. ** $P < 0.01$, *** $P < 0.001$. LV, lentivirus; miR, microRNA; NC, negative control; sh, short hairpin; RT-qPCR, reverse transcription-quantitative PCR.

Additionally, compared with tumors in the LV-sh NC1 + LV-sh NC2 group mice, Ki-67 expression in tumors in the LV-sh-YTHDF1 and LV-sh-LINC00900 group mice was decreased (Fig. 7F and G), whereas the proportion of TUNEL-positive cells was increased (Fig. 7H and I). These findings indicated that LINC00900 promoted GSC viability, invasion, self-renewal and tumor growth by regulating the miR-1205/STAT3 axis.

Discussion

Functional studies have shown that m6A regulator-mediated m6A modification serves a major role in glioma progression (28).

For example, the m6A methylase METTL3 enhances the stability of MALAT1 via m6A modification and activates NF- κ B to promote malignant progression of IDH-wildtype glioma (29). Furthermore, the m6A demethylase ALKBH5 maintains the tumorigenicity of GBM stem-like cells by sustaining FOXM1 expression and cell proliferation (30). The m6A reader YTHDF2 facilitates UBXL1 mRNA decay by recognizing METTL3-mediated m6A modification to activate NF- κ B and promote malignant progression of glioma (31). The present study investigated a glioma-related m6A regulator, the m6A-reading protein YTHDF1, which has been shown to increase glioma cell viability *in vitro* and promote tumor

formation *in vivo* (32). The present study observed increased expression of YTHDF1 in glioma tissues, which was consistent with a previous report (18). Moreover, it was revealed that the expression of YTHDF1 in GSCs was significantly higher than that in glioma cells. Overexpression of YTHDF1 promoted GSC viability, invasion and self-renewal, whereas knockdown of YTHDF1 expression inhibited GSC viability, invasion and self-renewal. These results suggested that YTHDF1 serves a role in the self-renewal and invasiveness of GSCs. The present study also assessed the molecular mechanism underlying the regulatory effects of YTHDF1 on the self-renewal and invasion of GSCs.

m6A affects the occurrence and development of tumors by regulating lncRNA expression (21). YTHDF proteins, including YTHDF1, YTHDF2 and YTHDF3, exhibit the same m6A-binding site in mRNA and co-mediate degradation of mRNA containing the m6A modification (33,34). YTHDF1 is highly expressed in GBM cells (35), and it positively regulates GBM cell proliferation, drug resistance and cancer stem cell-like characteristics (18). The present study showed that the expression levels of YTHDF1 in GSC-U87 and GSC-U251 cells was higher than those U87 and U251 cells, and overexpression of YTHDF1 promoted the viability, invasion and self-renewal of GSCs.

LINC00900 is a newly discovered lncRNA that is highly expressed in glioma, and is an m6A-related prognostic lncRNA of primary GBM (24). The present study revealed that LINC00900 was upregulated in glioma tissue, which is in agreement with a previous report (24). A total of 20 glioma tissues were collected, among which 16 patients had GBM (WHO grade IV) and 4 patients had astrocytoma (WHO grade III). To clarify differential expression of LINC00900 in tumor types, the 20 cancer tissues and adjacent tissues were divided into two groups by the tumor type, GBM and astrocytoma. In the future, the clinical sample size should be expanded for further analysis.

The present study also revealed that LINC00900 had a high level of m6A modification in glioma tissues. RIP and RNA pull-down assays showed that LINC00900 directly bound to YTHDF1. Actinomycin D treatment confirmed that YTHDF1 upregulated LINC00900 expression by maintaining its stability. Rescue experiments showed that LINC00900 knockdown significantly reversed the promoting effect of YTHDF1 on the viability, invasion and self-renewal of GSCs. Collectively, these results indicated that YTHDF1 upregulated the expression of LINC00900 by maintaining its stability, and promoted the viability and self-renewal of GSCs.

LncRNAs serve a carcinogenic role by acting as endogenous molecular sponges to compete with miRNA and affect target mRNA (36). For example, lncRNA BCYRN1 inhibits glioma tumorigenesis by competitively binding to miR-619-5p to regulate CUEDC2 expression (37). LncRNA PVT1 facilitates tumorigenesis and progression of glioma via regulation of the miR-128-3p/GREM1 axis (38). Notably, miR-1205 is downregulated in glioma tissues and cells, and multiple circular (circ)RNAs [circ-UBAP2 (39), circMAN2B2 (40), circ_0001982 (41) and circ_0034642 (42)] function as sponges of miR-1205 to promote glioma progression. Through bioinformatics prediction, a miR-1205-binding site was identified on the LINC00900 transcript. The results of a luciferase

reporter assay confirmed the target binding relationship between miR-1205 and LINC00900. Further rescue experiments showed that miR-1205 mimics significantly reversed the promoting effect of LINC00900 on the viability, invasion and self-renewal of GSCs. Thus, these results indicated that LINC00900 promotes the viability and self-renewal of GSCs by regulating miR-1205.

STAT3 is a member of the STAT protein family, and has an important role in transmitting signals from cytokines and growth factors (43). Activated STAT3 is associated with tumor occurrence and cancer progression by promoting the transcription of genes that control tumor cell viability, and inhibit apoptosis, vascularization and the cell cycle (44,45). For example, STAT3 promotes tumor progression in glioma by inducing FOXP1 transcription (46), and STAT3 inhibition promotes GBM cell apoptosis through MYC (47). In the present study, bioinformatics prediction revealed a miR-1205-binding site on the STAT3 3'-UTR. The results of a luciferase reporter assay confirmed the target binding relationship between miR-1205 and the STAT3 3'-UTR. Further rescue experiments showed that the miR-1205 mimics significantly reversed the enhancing effect of LINC00900 on STAT3 expression in GSCs. Taken together, these results indicated that LINC00900 upregulates STAT3 by sponging miR-1205.

In conclusion, the present study indicated that YTHDF1 promotes the viability, invasion and self-renewal of GSCs by regulating the LINC00900/miR-1205/STAT3 axis. Therefore, the YTHDF1/LINC00900/miR-1205/STAT3 axis may be a new therapeutic target for glioma.

Acknowledgements

Not applicable.

Funding

No funding was received.

Availability of data and materials

The data generated in the present study may be requested from the corresponding author.

Authors' contributions

YuZ and YiZ designed the research and drafted the manuscript. YuZ, YiZ, YaZ and ZL participated in the experiments. XZ performed the data analysis and revised the manuscript. YuZ and XZ confirm the authenticity of all the raw data. All authors read and approved the final manuscript.

Ethics approval and consent to participate

The ethics approval for studies on human tissue was approved by the Ethics Committee of Wuxi No. 2 People's Hospital (approval no. 2022-Y-116). All patients signed an informed consent form. The animal study was approved by the Medical Ethics Committee of Wuxi No. 2 People's Hospital (approval no. 2023-Y-200).

Patient consent for publication

Not applicable.

Competing interests

The authors declare that they have no competing interests.

References

- Xu S, Tang L, Li X, Fan F and Liu Z: Immunotherapy for glioma: Current management and future application. *Cancer Lett* 476: 1-12, 2020.
- Rong L, Li N and Zhang Z: Emerging therapies for glioblastoma: Current state and future directions. *J Exp Clin Cancer Res* 41: 142, 2022.
- Ma Q, Long W, Xing C, Chu J, Luo M, Wang HY, Liu Q and Wang RF: Cancer stem cells and immunosuppressive microenvironment in glioma. *Front Immunol* 9: 2924, 2018.
- Zhao LY, Song J, Liu Y, Song CX and Yi C: Mapping the epigenetic modifications of DNA and RNA. *Protein Cell* 11: 792-808, 2020.
- Fu Y, Dominissini D, Rechavi G and He C: Gene expression regulation mediated through reversible m⁶A RNA methylation. *Nat Rev Genet* 15: 293-306, 2014.
- Du J, Ji H, Ma S, Jin J, Mi S, Hou K, Dong J, Wang F, Zhang C, Li Y and Hu S: m⁶A regulator-mediated methylation modification patterns and characteristics of immunity and stemness in low-grade glioma. *Brief Bioinform* 22: bbab013, 2021.
- Tao N, Wen T, Li T, Luan L, Pan H and Wang Y: Interaction between m⁶A methylation and noncoding RNA in glioma. *Cell Death Discov* 8: 283, 2022.
- Cui Q, Shi H, Ye P, Li L, Qu Q, Sun G, Sun G, Lu Z, Huang Y, Yang CG, *et al*: m(6)A RNA methylation regulates the self-renewal and tumorigenesis of glioblastoma stem cells. *Cell Rep* 18: 2622-2634, 2017.
- Visvanathan A, Patil V, Arora A, Hegde AS, Arivazhagan A, Santosh V and Somasundaram K: Essential role of METTL3-mediated m(6)A modification in glioma stem-like cells maintenance and radioresistance. *Oncogene* 37: 522-533, 2018.
- Shi J, Zhang P, Dong X, Yuan J, Li Y, Li S, Cheng S, Ping Y, Dai X and Dong J: METTL3 knockdown promotes temozolomide sensitivity of glioma stem cells via decreasing MGMT and APNG mRNA stability. *Cell Death Discov* 9: 22, 2023.
- You J, Tao B, Peng L, Peng T, He H, Zeng S, Han J, Chen L, Xia X, Yang X and Zhong C: Transcription factor YY1 mediates self-renewal of glioblastoma stem cells through regulation of the SENP1/METTL3/MYC axis. *Cancer Gene Ther* 30: 683-693, 2023.
- Sun Y, Dong D, Xia Y, Hao L, Wang W and Zhao C: YTHDF1 promotes breast cancer cell growth, DNA damage repair and chemoresistance. *Cell Death Discov* 13: 230, 2022.
- He Y, Wang W, Xu X, Yang B, Yu X, Wu Y and Wang J: Mettl3 inhibits the apoptosis and autophagy of chondrocytes in inflammation through mediating Bcl2 stability via Ythdf1-mediated m⁶A modification. *Bone* 154: 116182, 2022.
- Lin Z, Niu Y, Wan A, Chen D, Liang H, Chen X, Sun L, Zhan S, Chen L, Cheng C, *et al*: RNA m⁶A methylation regulates sorafenib resistance in liver cancer through FOXO3-mediated autophagy. *EMBO J* 39: e103181, 2020.
- Liu T, Wei Q, Jin J, Luo Q, Liu Y, Yang Y, Cheng C, Li L, Pi J, Si Y, *et al*: The m⁶A reader YTHDF1 promotes ovarian cancer progression via augmenting EIF3C translation. *Nucleic Acids Res* 48: 3816-3831, 2020.
- Wang S, Gao S, Zeng Y, Zhu L, Mo Y, Wong CC, Bao Y, Su P, Zhai J, Wang L, *et al*: N⁶-Methyladenosine reader YTHDF1 promotes ARHGEF2 translation and RhoA signaling in colorectal cancer. *Gastroenterology* 162: 1183-1196, 2022.
- Deng X, Sun X, Hu Z, Wu Y, Zhou C, Sun J, Gao X and Huang Y: Exploring the role of m⁶A methylation regulators in glioblastoma multiforme and their impact on the tumor immune microenvironment. *FASEB J* 37: e23155, 2023.
- Yarmishyn AA, Yang YP, Lu KH, Chen YC, Chien Y, Chou SJ, Tsai PH, Ma HI, Chien CS, Chen MT and Wang ML: Musashi-1 promotes cancer stem cell properties of glioblastoma cells via upregulation of YTHDF1. *Cancer Cell Int* 20: 597, 2020.
- Jiang MC, Ni JJ, Cui WY, Wang BY and Zhuo W: Emerging roles of lncRNA in cancer and therapeutic opportunities. *Am J Cancer Res* 9: 1354-1366, 2019.
- Meyer KD, Saletore Y, Zumbo P, Elemento O, Mason CE and Jaffrey SR: Comprehensive analysis of mRNA methylation reveals enrichment in 3' UTRs and near stop codons. *Cell* 149: 1635-1646, 2012.
- Huang H, Weng H and Chen J: m(6)a modification in coding and non-coding RNAs: Roles and therapeutic implications in cancer. *Cancer Cell* 37: 270-288, 2020.
- Liu P, Fan B, Othmane B, Hu J, Li H, Cui Y, Ou Z, Chen J and Zu X: m⁶A-induced lncDBET promotes the malignant progression of bladder cancer through FABP5-mediated lipid metabolism. *Theranostics* 12: 6291-6307, 2022.
- Li ZX, Zheng ZQ, Yang PY, Lin L, Zhou GQ, Lv JW, Zhang LL, Chen F, Li YQ, Wu CF, *et al*: WTAP-mediated m⁶A modification of lncRNA DIAPH1-AS1 enhances its stability to facilitate nasopharyngeal carcinoma growth and metastasis. *Cell Death Differ* 29: 1137-1151, 2022.
- Wang W, Li J, Lin F, Guo J and Zhao J: Identification of N(6)-methyladenosine-related lncRNAs for patients with primary glioblastoma. *Neurosurg Rev* 44: 463-470, 2021.
- Liu H, Xu Y, Yao B, Sui T, Lai L and Li Z: A novel N⁶-methyladenosine (m⁶A)-dependent fate decision for the lncRNA THOR. *Cell Death Dis* 11: 613, 2020.
- Wu W, Klockow JL, Zhang M, Lafortune F, Chang E, Jin L, Wu Y and Daldrop-Link HE: Glioblastoma multiforme (GBM): An overview of current therapies and mechanisms of resistance. *Pharmacol Res* 171: 105780, 2021.
- Livak KJ and Schmittgen TD: Analysis of relative gene expression data using real-time quantitative PCR and the 2(-Delta Delta C(T)) method. *Methods* 25: 402-408, 2001.
- Zhang G, Zheng P, Lv Y, Shi Z and Shi F: m⁶A regulatory gene-mediated methylation modification in glioma survival prediction. *Front Genet* 13: 873764, 2022.
- Chang YZ, Chai RC, Pang B, Chang X, An SY, Zhang KN, Jiang T and Wang YZ: METTL3 enhances the stability of MALAT1 with the assistance of HuR via m⁶A modification and activates NF-κB to promote the malignant progression of IDH-wildtype glioma. *Cancer Lett* 511: 36-46, 2021.
- Zhang S, Zhao BS, Zhou A, Lin K, Zheng S, Lu Z, Chen Y, Sulman EP, Xie K, Böglér O, *et al*: m(6)A demethylase ALKBH5 maintains tumorigenicity of glioblastoma stem-like cells by sustaining FOXM1 expression and cell proliferation program. *Cancer Cell* 31: 591-606.e596, 2017.
- Chai RC, Chang YZ, Chang X, Pang B, An SY, Zhang KN, Chang YH, Jiang T and Wang YZ: YTHDF2 facilitates UBXM1 mRNA decay by recognizing METTL3-mediated m(6)A modification to activate NF-κB and promote the malignant progression of glioma. *J Hematol Oncol* 14: 109, 2021.
- Xu C, Yuan B, He T, Ding B and Li S: Prognostic values of YTHDF1 regulated negatively by mir-3436 in glioma. *J Cell Mol Med* 24: 7538-7549, 2020.
- Zaccara S and Jaffrey S: A unified model for the function of YTHDF proteins in regulating m⁶A-modified mRNA. *Cell* 181: 1582-1595.e1518, 2020.
- Zou Z, Sepich-Poore C, Zhou X, Wei J and He C: The mechanism underlying redundant functions of the YTHDF proteins. *Genome Biol* 24: 17, 2023.
- Cong P, Wu T, Huang X, Liang H, Gao X, Tian L, Li W, Chen A, Wan H, He M, *et al*: Identification of the role and clinical prognostic value of target genes of m⁶A RNA methylation regulators in glioma. *Front Cell Dev Biol* 9: 709022, 2021.
- Liu G, Li H, Ji W, Gong H, Jiang Y, Ji G and Liu G: Construction of a ceRNA network in glioma and analysis of its clinical significance. *BMC Genomics* 22: 722, 2021.
- Mu M, Niu W, Zhang X, Hu S and Niu C: lncRNA BCYRN1 inhibits glioma tumorigenesis by competitively binding with miR-619-5p to regulate CUEDC2 expression and the PTEN/AKT/p21 pathway. *Oncogene* 39: 6879-6892, 2020.
- Fu C, Li D, Zhang X, Liu N, Chi G and Jin X: lncRNA PVT1 facilitates tumorigenesis and progression of glioma via regulation of miR-128-3p/GREMI axis and BMP signaling pathway. *Neurotherapeutics* 15: 1139-1157, 2018.
- Wang J, Li T and Wang B: Circ-UBAP2 functions as sponges of miR-1205 and miR-382 to promote glioma progression by modulating STC1 expression. *Cancer Med* 10: 1815-1828, 2021.

40. Xiong J, Wang T, Tang H, Lv Z and Liang P: Circular RNA circMAN2B2 facilitates glioma progression by regulating the miR-1205/S100A8 axis. *J Cell Physiol* 234: 22996-23004, 2019.
41. Ma Z, Ma J, Lang B, Xu F, Zhang B and Wang X: Circ_0001982 up-regulates the expression of E2F1 by adsorbing miR-1205 to facilitate the progression of glioma. *Mol Biotechnol* 65: 466-476, 2023.
42. Yang M, Li G, Fan L, Zhang G, Xu J and Zhang J: Circular RNA circ_0034642 elevates BATF3 expression and promotes cell proliferation and invasion through miR-1205 in glioma. *Biochem Biophys Res Commun* 508: 980-985, 2019.
43. Hirano T, Ishihara K and Hibi M: Roles of STAT3 in mediating the cell growth, differentiation and survival signals relayed through the IL-6 family of cytokine receptors. *Oncogene* 19: 2548-2556, 2000.
44. Zou S, Tong Q, Liu B, Huang W, Tian Y and Fu X: Targeting STAT3 in cancer immunotherapy. *Mol Cancer* 19: 145, 2020.
45. Lee H, Jeong AJ and Ye SK: Highlighted STAT3 as a potential drug target for cancer therapy. *BMB Rep* 52: 415-423, 2019.
46. Sun X, Wang J, Huang M, Chen T, Chen J, Zhang F, Zeng H, Xu Z and Ke Y: STAT3 promotes tumour progression in glioma by inducing FOXP1 transcription. *J Cell Mol Med* 22: 5629-5638, 2018.
47. Wang H, Tao Z, Feng M, Li X, Deng Z, Zhao G, Yin H, Pan T, Chen G, Feng Z, *et al*: Dual PLK1 and STAT3 inhibition promotes glioblastoma cells apoptosis through MYC. *Biochem Biophys Res Commun* 533: 368-375, 2020.



Copyright © 2024 Zhang et al. This work is licensed under a Creative Commons Attribution-NonCommercial-NoDerivatives 4.0 International (CC BY-NC-ND 4.0) License.